Numerical results of Crank-Nicolson scheme on unsteady nano fluid under the effect of Prandtl, Mixed Convection, and Magnetohydrodynamics

Mohammad Ghani, Yolanda Norasia, Indira Anggriani, Mohamad Tafrikan, Zulaikha

***Abstract*—In this paper, we are interested in the numerical results on the temperature and velocity profiles over a sphere of unsteady nano fluid by dealing with the effect of Prandtl, mixed convection, and magnetohydrodynamics. We first employ the boundary layer theory to establish the continuity, momentum, and energy equations. We further solve those differential equations numerically by using the finite difference scheme of Crank-Nicolson and Thomas algorithm for the iteration technique. The temperature and velocity profiles are established graphically for the variations of Prandtl, mixed convection, and magnetohydrodynamics. The velocity profile decreases when the variations of Prandtl numbers increase. Moreover, the velocity profiles increase when the variations of mixed convection and magnetohydrodynamics are increased. The temperature profiles are decreased for all variations of Prandtl numbers, mixed convection and magnetohydrodynamics.**

***Index Terms*—unsteady nano fluid, Crank-Nicolson scheme, Prandtl numbers, mixed convection and magnetohydrodynamics.**

I. Introduction

FLUID flow modeling is an applied science of mathematics in engineering and industry. Flow modeling is based on the application of physical laws which are then adjusted to real problems. These laws are in the form of the law of conservation of mass, Newton-II law, and the Law of Thermodynamics-I [1]. The law of conservation of mass is applied with regard to the density of the fluid. Density is based on the particles in a fluid. Collision particles cause momentum according to Newton's second law. Collisions between particles produce energy according to the First Law of Thermodynamics. The equations formed are then converted into non-dimensional equations and similarity equations [2].

Nanoparticles have the ability to increase thermal conductivity. The particles added to the base fluid are called nanofluids [3]. Nanofluids are categorized as non-Newtonian fluids. Research related to nanofluids was carried out by [4] on the effect of Magnetohydrodynamics on the flow of nanofluids through a porous cylinder. The research shows that the magnetic effect causes the flow velocity to decrease and the fluid temperature to increase. Subsequent research [5] regarding the effect of nanoparticles in the form of metals and metal oxides on the flow of MHD nanofluids. The results showed that nanoarticles in the form of metal oxides increased the fluid flow temperature faster. Research on the effect of nanoparticles in the form of Argentum metal (Ag) on fluid flow through solid balls was carried out by [6]. The flow velocity decreases due to magnetic variations. On the other hand, the fluid temperature increases due to magnetic variations. This happens because the more significant the magnetic variation, the more nanoparticles increase. The effect of heat generation and thermal radiation on nanofluids flow was used in [7], [8]. Maxwell nanofluid flow with Copper (Cu) and Titanium (Ti) nanoparticles were carried out [9], and it was found that the volume fraction affects the fluid temperature. The numerical solution for this research was carried out using the Runge-Kutta method. Prameela et all analyzed the effect of Prandtl number in fluid flow. They conclude that velocity and temperature profile increase with an increase in Prandtl number [10]. Recently, the problems of heat, slip flow, and thermal radiation of ferrofluid for various of geometry such as the stagnation point stretching/shrinking surface have been extensively studied in [11], [12].

The Prandl number (Pr) is the ratio between the momentum diversity and the heat used to determine the temperature of the fluid flow. Prandtl number has a inverse linear relationship with temperature of fluid [13]. Based on the influence of nanoparticles in the temperature distribution, this study discusses the effect of the Prantdl number and mixed convection on the flow velocity and fluid temperature. According to some previous investigations, we study the numerical results of mixed convection problem through a solid sphere by employing the unconditionally stable method of Crank-Nicolson, where these finite difference approximations are then iterated by the Thomas algorithm. In this paper, we are not interested in the stream function of boundary layer near stagnation point as in [14] but only the non-dimensional coupled differential equations. Then, the strategy of numerical simulation is adapted from [15], by applying the Crank-Nicolson scheme.

We further organize this paper as follows. In Section 2, we present the mathematical model, which is adapted from the physical model and boundary layer theory of nano fluid through a sphere. We further give the finite difference scheme to the non-dimensional governing equations and the numerical simulations for the finite difference approximations. In Section 3, we give some conclusions based on the results and

M. Ghani is with the Faculty of Advanced Technology and Multidiscipline, Universitas Airlangga, Indonesia email: mohammad.ghani@ftmm.unair.ac.id

Y. Norasia is with the Department of Mathematics, UIN Walisongo, Indonesia email: yolandanorasia@walisongo.ac.id

I. Anggriani is with the Department of Mathematics, Institut Teknologi Kalimantan, Indonesia email: indira@lecturer.itk.ac.id

M. Tafrikan is with the Department of Mathematics, UIN Walisongo, Indonesia email: tafrikan@walisongo.ac.id

Zulaikha is with the Department of Mathematics, UIN Walisongo, Indonesia email: zulaikha@walisongo.ac.id

Manuscript received August 19, 2022; accepted September 2, 2022.

discussions obtained in the previous section.

II. Main Results

In this section, we first present the mathematical model of continuity, momentum, and energy which are derived from the law of mass conservation, the second law of Newton, and the first law of thermodynamics respectively. Then, we employ the numerical method of Crank-Nicolson to the non-dimensional governing equations and the Thomas algorithm to establish the numerical results iteratively by using software MATLAB R2013a.

A. Mathematical Model

We consider the mixed convection through a sphere of unsteady nano fluid with the effect of magnetohydrodynamics. The physical model of this paper is represented in Figure 1. The Figure 1 presents the illustration of the physical model and coordinate system of the problem. The nano fluid before passing through a sphere has the velocity U_∞ and temperature T_∞. This current paper, we only focus on the sphere which does not have porosity. So, the nano fluid only passes through the surface of the sphere and the velocity at the z-axis is not considered. Due to the friction between the nano fluid and the surface of a sphere, the magnetohydrodynamics and mixed convection of a sphere affect the velocity and temperature profiles of nano fluid.

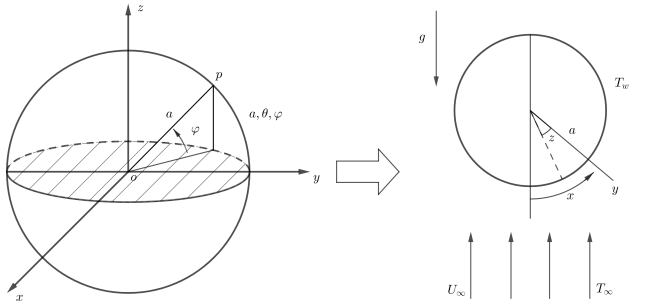

Fig. 1. Coordinate System of Sphere

The phenomena of nano fluid flow over a solid sphere in Figure 1 can be stated in the coupled differential equations, which are derived from the following dimensional continuity, momentum, and energy equations.

1) Dimensional Continuity Equation:

$$\frac{\partial(\bar{r}\bar{u})}{\partial\bar{x}} + \frac{\partial(\bar{r}\bar{v})}{\partial\bar{y}} = 0. \tag{1}$$

2) Dimensional Momentum Equation:

$$\rho_{fn}\left(\frac{\partial\bar{u}}{\partial\bar{t}} + \bar{u}\frac{\partial\bar{u}}{\partial\bar{x}} + \bar{v}\frac{\partial\bar{u}}{\partial\bar{y}}\right) = -\frac{\partial\bar{p}}{\partial\bar{x}} + \mu_{fn}\left(\frac{\partial^2\bar{u}}{\partial\bar{x}^2} + \frac{\partial^2\bar{u}}{\partial\bar{y}^2}\right) + \sigma(B_0)^2\bar{u} + (\rho_{fn} - \rho_\infty)g_{\bar{x}}, \tag{2}$$

$$\rho_{fn}\left(\frac{\partial\bar{v}}{\partial\bar{t}} + \bar{u}\frac{\partial\bar{v}}{\partial\bar{x}} + \bar{v}\frac{\partial\bar{v}}{\partial\bar{y}}\right) = -\frac{\partial\bar{p}}{\partial\bar{y}} + \mu_{fn}\left(\frac{\partial^2\bar{v}}{\partial\bar{x}^2} + \frac{\partial^2\bar{v}}{\partial\bar{y}^2}\right) + \sigma(B_0)^2\bar{v} + (\rho_{fn} - \rho_\infty)g_{\bar{y}}, \tag{3}$$

where the dimensional variables of $\bar{x}, \bar{y}$ are the cartesian coordinate system. Moreover, the dimensional variables of $\bar{u}, \bar{v}$ are related to the velocity of fluid moving in the $\bar{x}, \bar{y}$, and $\bar{r}$ is the radial distance of sphere which has been derived more detail from the previous study (see [16], Appendix).

3) Dimensional Energy Equation:

$$\frac{\partial\bar{T}}{\partial\bar{t}} + \bar{u}\frac{\partial\bar{T}}{\partial\bar{x}} + \bar{v}\frac{\partial\bar{T}}{\partial\bar{y}} = \alpha_{fn}\left(\frac{\partial^2\bar{T}}{\partial\bar{x}^2} + \frac{\partial^2\bar{T}}{\partial\bar{y}^2}\right). \tag{4}$$

The continuity, momentum, and energy equations of (1)-(4) satisfy the following initial and boundary conditions

$$\begin{aligned} &\bar{t} = 0 : \bar{u} = \bar{v} = 0, \bar{T} = T_\infty \text{ for every } \bar{x}, \bar{y} \\ &\bar{t} > 0 : \bar{u} = \bar{v} = 0, \bar{T} = T_w \text{ at } \bar{y} = 0 \\ &\qquad \bar{u} = \bar{u}_e(\bar{x}), \bar{u} = \bar{v}, \bar{T} = T_\infty \text{ at } \bar{y} \to \infty. \end{aligned} \tag{5}$$

Then, we simplify the above dimensional governing equations to be dimensional equations by employing the following non-dimensional variables

$$\begin{aligned} &x = \frac{\bar{x}}{a}; y = Re^{\frac{1}{2}}\frac{\bar{y}}{a}; t = \frac{U_\infty\bar{t}}{a}; u = \frac{\bar{u}}{U_\infty}; v = Re^{\frac{1}{2}}\frac{\bar{v}}{U_\infty}; \\ &T = \frac{\bar{T} - T_\infty}{T_w - T_\infty}; p = \frac{\bar{p}}{\rho_{fn}U_\infty^2}; r(x) = \frac{\bar{r}(\bar{x})}{a}; u_e(x) = \frac{\bar{u}_e(x)}{U_\infty}; \end{aligned} \tag{6}$$

where
Re : Reynolds Number, $Re = \frac{U_\infty a}{v_{fn}}$,
v_{fn} : Kinematic Viscosity of Nano Fluid,
μ_{fn} : Viscosity of Nano Fluid,
ρ_{fn} : Density of Nano Fluid,
p : Pressure,
and the gravity is defined as follows

$$g_{\bar{x}} = -g\ sin\left(\frac{\bar{x}}{a}\right), \quad g_{\bar{y}} = g\ cos\left(\frac{\bar{x}}{a}\right). \tag{7}$$

We further substitute the non-dimensional variables (6) and (7) into the dimensional governing equations, initial, and boundary conditions (1)-(5) to get the following non-dimensional governing equations.

4) Non-Dimensional Continuity Equation:

$$\frac{\partial(ru)}{\partial x} + \frac{\partial(rv)}{\partial y} = 0, \tag{8}$$

5) Non-Dimensional Momentum Equation:

$$\frac{\partial u}{\partial t} + u\frac{\partial u}{\partial x} + v\frac{\partial u}{\partial y} = -\frac{\partial p}{\partial x} + \frac{v_{fn}}{Rev_f}\frac{\partial^2 u}{\partial x^2} + \frac{v_{fn}}{v_f}\frac{\partial^2 u}{\partial y^2} + Mu + \lambda T sin(x), \tag{9}$$

$$\frac{1}{Re}\left(\frac{\partial v}{\partial t}+u\frac{\partial v}{\partial x}+v\frac{\partial v}{\partial y}\right)=-\frac{\partial p}{\partial y}+\frac{v_{fn}}{v_f}\frac{1}{Re^2}\frac{\partial^2 v}{\partial x^2}+\frac{v_{fn}}{v_f}\frac{1}{Re}\frac{\partial^2 v}{\partial y^2}+\frac{M}{Re}v-\frac{\lambda}{Re^{1/2}}Tcos(x), \quad (10)$$

6) Non-Dimensional Energy Equation:

$$\frac{\partial T}{\partial t}+u\frac{\partial T}{\partial x}+v\frac{\partial T}{\partial y}=\frac{1}{Re}\frac{1}{Pr}\frac{\alpha_{fn}}{\alpha_f}\frac{\partial^2 T}{\partial x^2}+\frac{1}{Pr}\frac{\alpha_{fn}}{\alpha_f}\frac{\partial^2 T}{\partial y^2}, \quad (11)$$

The continuity, momentum, and energy equations of (8)-(11) satisfy the following initial and boundary conditions

$$\begin{aligned} &t=0: u=v=0, T=0 \text{ for every } x,y\\ &t>0: u=v=0, T=1 \text{ at } y=0\\ &\quad u=u_e(x), T=0 \text{ at } y\longrightarrow\infty. \end{aligned} \quad (12)$$

B. Boundary Layer Theory

The Boundary layer is part of the fluid mechanics problem which is a layer formed because of friction between nano fluid passing through the surface of the solid sphere caused by the viscosity of the nano fluid. Based on the non-dimensional governing equations (8)-(11), we can derive new governing equations by employing the boundary layer approach. Since the boundary layer is very thin, then the limit of $\frac{1}{R_e}$ goes to zero, as $R_e\to\infty$, one has

1) Continuity Equation:

$$\frac{\partial(ru)}{\partial x}+\frac{\partial(rv)}{\partial y}=0, \quad (13)$$

2) Momentum Equation:

$$\frac{\partial u}{\partial t}+u\frac{\partial u}{\partial x}+v\frac{\partial u}{\partial y}=-\frac{\partial p}{\partial x}+\frac{v_{fn}}{v_f}\frac{\partial^2 u}{\partial y^2}+Mu+\lambda T sin(x), \quad (14)$$

and

$$-\frac{\partial p}{\partial y}=0.$$

3) Energy Equation:

$$\frac{\partial T}{\partial t}+u\frac{\partial T}{\partial x}+v\frac{\partial T}{\partial y}=\frac{1}{Pr}\frac{\alpha_{fn}}{\alpha_f}\frac{\partial^2 T}{\partial y^2}, \quad (15)$$

In this study, the type of fluid is nano fluid. Therefore, the above non-dimensional governing equation is brought into the form of nano fluid by substituting the following variables which have the correlations between nano fluid and basic fluid.

Density of Nano Fluid : $\rho_{fn}=(1-\chi)\rho_f+\chi\rho_s$.

Viscosity : $\mu_{fn}=\frac{\mu_f}{(1-\chi)^{2.5}}$.

Specific Heat of Nano Fluid :
$(\rho C_p)_{fn}=(1-\chi)(\rho C_p)_f+\chi(\rho C_p)_s$.

Thermal Conductivity :
$$\frac{k_{fn}}{k_f}=\frac{(k_s+2k_f)-2\chi(k_f-k_s)}{(k_s+2k_f)+\chi(k_f-k_s)}.$$

Then, we substitute the variables of nano fluid into (13)-(15) to get the following new non-dimensional coupled differential equations.

$$\frac{\partial(ru)}{\partial x}+\frac{\partial(rv)}{\partial y}=0, \quad (16)$$

$$\frac{\partial u}{\partial t}+u\frac{\partial u}{\partial x}+v\frac{\partial u}{\partial y}=-\frac{\partial p}{\partial x}+\frac{1}{(1-\chi)^{2.5}\left((1-\chi)+\chi\left(\frac{\rho_s}{\rho_f}\right)\right)}\frac{\partial^2 u}{\partial y^2}+Mu+\lambda T\, sin(x), \quad (17)$$

$$\frac{\partial T}{\partial t}+u\frac{\partial T}{\partial x}+v\frac{\partial T}{\partial y}=\frac{1}{Pr}\left(\frac{(k_s+2k_f)-2\chi(k_f-k_s)}{((k_s+2k_f)+\chi(k_f-k_s))\left((1-\chi)+\left(\frac{\chi(\rho C_p)_s}{(\rho c_p)_f}\right)\right)}\right)\frac{\partial^2 T}{\partial y^2}. \quad (18)$$

Based on the momentum equation (16), we can define the following velocity of free stream in a sphere

$$u_e=\frac{3}{2}\, sin(x), \quad (19)$$

which gives

$$\frac{\partial u_e}{\partial t}=0; \frac{\partial u_e}{\partial y}=0; \frac{\partial^2 u_e}{\partial y^2}=0,$$

and

$$u_e\frac{\partial u_e}{\partial x}=-\frac{\partial p}{\partial x}+Mu_e+\lambda T\, sin(x).$$

Since the non-dimensional momentum equation (17) satisfy the initial and boundary conditions defined in (12). Then, at $y\to\infty$, $T=0$ which implies that

$$-\frac{\partial p}{\partial x}=u_e\frac{\partial u_e}{\partial x}-Mu_e. \quad (20)$$

We finally substitute (20) into (17) to get the following new non-dimensional momentum equation.

$$\frac{\partial u}{\partial t}+u\frac{\partial u}{\partial x}+v\frac{\partial u}{\partial y}=u_e\frac{\partial u_e}{\partial x}+\frac{1}{(1-\chi)^{2.5}\left((1-\chi)+\chi\left(\frac{\rho_s}{\rho_f}\right)\right)}\frac{\partial^2 u}{\partial y^2}+M(u-u_e)+\lambda T\, sin(x). \quad (21)$$

C. Numerical Analysis

We are interested in non-dimensional governing equations in coupled non-dimensional equations with boundary and initial

conditions. Since the analytical solution is extremely difficult to establish, we use the finite difference method to approximate the non-dimensional governing equations. In this paper, we use the Crank-Nicolson implicit finite difference method, which is unconditionally stable. This Crank-Nicolson method is used to solve equations (16), (18), and (21) with the initial and boundary conditions given by (12).

We divide the region of this problem into the grid of lines parallel to x-axis and y-axis to get the difference equations of (16), (18), and (21), where x-axis is along with the surface of sphere and y-axis is normal to the surface of sphere. We denote u^{n+1}, v^{n+1}, and T^{n+1} as the next step of time for u, v, and T respectively.

1) Finite difference of first order derivative:

$$\begin{aligned}
&\left(\frac{\partial u}{\partial t}\right)_{i,j} = \frac{u_{i,j}^{n+1} - u_{i,j}^{n}}{\Delta t}; \left(\frac{\partial T}{\partial t}\right)_{i,j} = \frac{T_{i,j}^{n+1} - T_{i,j}^{n}}{\Delta t};\\
&\left(\frac{\partial u}{\partial y}\right)_{i,j} = \frac{u_{i,j} - u_{i,j-1}}{\Delta y}; \left(\frac{\partial v}{\partial y}\right)_{i,j} = \frac{v_{i,j} - v_{i,j-1}}{\Delta y};\\
&\left(\frac{\partial T}{\partial y}\right)_{i,j} = \frac{T_{i,j} - T_{i,j-1}}{\Delta y}; \left(\frac{\partial u}{\partial y}\right)_{i,j} = \frac{u_{i,j+1} - u_{i,j-1}}{2\Delta y};\\
&\left(\frac{\partial v}{\partial y}\right)_{i,j} = \frac{v_{i,j+1} - v_{i,j-1}}{2\Delta y}; \left(\frac{\partial T}{\partial y}\right)_{i,j} = \frac{T_{i,j+1} - T_{i,j-1}}{2\Delta y};\\
&\left(\frac{\partial u}{\partial x}\right)_{i,j} = \frac{u_{i,j} - u_{i-1,j}}{\Delta x}; \left(\frac{\partial v}{\partial x}\right)_{i,j} = \frac{v_{i,j} - v_{i-1,j}}{\Delta x};\\
&\left(\frac{\partial T}{\partial x}\right)_{i,j} = \frac{T_{i,j} - T_{i-1,j}}{\Delta x},
\end{aligned} \tag{22}$$

2) Finite difference of second order derivative:

$$\begin{aligned}
\left(\frac{\partial^2 u}{\partial y^2}\right)_{i,j} &= \frac{u_{i,j+1} - 2u_{i,j} + u_{i,j-1}}{(\Delta y)^2};\\
\left(\frac{\partial^2 T}{\partial y^2}\right)_{i,j} &= \frac{T_{i,j+1} - 2T_{i,j} + T_{i,j-1}}{(\Delta y)^2},
\end{aligned} \tag{23}$$

where the subscripts i, j and superscript n respectively present the x-axis, y-axis, and the time variable of t. We substitute the above finite difference approximation into non-dimensional coupled differential equations (16), (18), and (21), then one has the following finite difference equations

$$\begin{aligned}
&\frac{1}{2\Delta x}\left(u_{i,j}^{n+1} - u_{i-1,j}^{n+1} + u_{i,j}^{n} - u_{i-1,j}^{n}\right) +\\
&\frac{1}{2\Delta x}\left(u_{i,j-1}^{n+1} - u_{i-1,j-1}^{n+1} + u_{i,j-1}^{n} - u_{i-1,j-1}^{n}\right) +\\
&\frac{1}{\Delta y}\left(v_{i,j}^{n+1} - v_{i,j-1}^{n+1} + v_{i,j}^{n} - v_{i,j-1}^{n}\right) +\\
&\left(u_{i,j}^{n+1} + u_{i,j}^{n}\right) cot\left(x\right) = 0.
\end{aligned} \tag{24}$$

$$\begin{aligned}
&\frac{1}{\Delta t}\left(u_{i,j}^{n+1} - u_{i,j}^{n}\right) + \frac{u_{i,j}^{n}}{2\Delta x}\left(u_{i,j}^{n+1} - u_{i-1,j}^{n+1} + u_{i,j}^{n} - u_{i-1,j}^{n}\right) +\\
&\frac{v_{i,j}^{n}}{4\Delta y}\left(u_{i,j+1}^{n+1} - u_{i,j-1}^{n+1} + u_{i,j+1}^{n} - u_{i,j-1}^{n}\right) =\\
&\frac{\mathcal{L}}{2(\Delta y)^2}\left(u_{i,j-1}^{n+1} - 2u_{i,j}^{n+1} + u_{i,j+1}^{n+1} + u_{i,j-1}^{n} - 2u_{i,j}^{n} + u_{i,j+1}^{n}\right) +\\
&\frac{9}{4}\, sin(x(i))cos(x(i)) + \frac{M}{2}(u_{i,j}^{n+1} + u_{i,j}^{n}) -\\
&\frac{3M}{2}\, sin(x(i)) + \frac{\lambda}{2}(T_{i,j}^{n+1} + T_{i,j}^{n})\, sin(x(i)).
\end{aligned} \tag{25}$$

$$\begin{aligned}
&\frac{1}{\Delta t}\left(T_{i,j}^{n+1} - T_{i,j}^{n}\right) + \frac{u_{i,j}^{n}}{2\Delta x}\left(T_{i,j}^{n+1} - T_{i-1,j}^{n+1} + T_{i,j}^{n} - T_{i-1,j}^{n}\right) +\\
&\frac{v_{i,j}^{n}}{4\Delta y}\left(T_{i,j+1}^{n+1} - T_{i,j-1}^{n+1} + T_{i,j+1}^{n} - T_{i,j-1}^{n}\right) =\\
&\frac{\mathcal{K}}{2P_r(\Delta y)^2}\left(T_{i,j-1}^{n+1} - 2T_{i,j}^{n+1} + T_{i,j+1}^{n+1} + T_{i,j-1}^{n} - 2T_{i,j}^{n} + T_{i,j+1}^{n}\right).
\end{aligned} \tag{26}$$

By rearranging the finite difference equations (24)-(26), one can derive

$$\begin{aligned}
v_{i,j}^{n+1} = {} & v_{i,j-1}^{n+1} - v_{i,j}^{n} + v_{i,j-1}^{n} -\\
& \mathcal{A}\begin{pmatrix} u_{i,j}^{n+1} - u_{i-1,j}^{n+1} + u_{i,j}^{n} - u_{i-1,j}^{n} + \\ u_{i,j-1}^{n+1} - u_{i-1,j-1}^{n+1} + u_{i,j-1}^{n} - u_{i-1,j-1}^{n} \end{pmatrix} -\\
& \Delta y\left(u_{i,j}^{n+1} + u_{i,j}^{n}\right) cot\left(x(i)\right),
\end{aligned} \tag{27}$$

$$\begin{aligned}
&(-\mathcal{B}_2 - \mathcal{B}_3)u_{i,j-1}^{n+1} + (1 + \mathcal{B}_1 + 2\mathcal{B}_3 - \mathcal{B}_5)u_{i,j}^{n+1} +\\
&(\mathcal{B}_2 - \mathcal{B}_3)u_{i,j+1}^{n+1} = (1 + \mathcal{B}_5)u_{i,j}^{n} + \mathcal{B}_1(u_{i-1,j}^{n+1} + u_{i-1,j}^{n} - u_{i,j}^{n}) +\\
&\qquad \mathcal{B}_2(u_{i,j-1}^{n} - u_{i,j+1}^{n}) +\\
&\qquad \mathcal{B}_3(u_{i,j-1}^{n} - 2u_{i,j}^{n} + u_{i,j+1}^{n}) +\\
&\qquad \mathcal{B}_4 - \mathcal{B}_6 + \mathcal{B}_7(T_{i,j}^{n+1} + T_{i,j}^{n}),
\end{aligned} \tag{28}$$

$$\begin{aligned}
&(-\mathcal{C}_2 - \mathcal{C}_3)T_{i,j-1}^{n+1} + (1 + \mathcal{C}_1 + 2\mathcal{C}_3)T_{i,j}^{n+1} +\\
&(\mathcal{C}_2 - \mathcal{C}_3)T_{i,j+1}^{n+1} = T_{i,j}^{n} + \mathcal{C}_1(T_{i-1,j}^{n+1} + T_{i-1,j}^{n} - T_{i,j}^{n}) +\\
&\qquad \mathcal{C}_2(T_{i,j-1}^{n} - T_{i,j+1}^{n}) +\\
&\qquad \mathcal{C}_3(T_{i,j-1}^{n} - 2T_{i,j}^{n} + T_{i,j+1}^{n}),
\end{aligned} \tag{29}$$

where

$$\begin{aligned}
&\mathcal{A} = \frac{\Delta y}{2\Delta x}; \mathcal{B}_1 = \mathcal{C}_1 = \frac{u_{i,j}^{n}\Delta t}{2\Delta x}; \mathcal{B}_2 = \mathcal{C}_2 = \frac{v_{i,j}^{n}\Delta t}{4\Delta y};\\
&\mathcal{B}_3 = \frac{\mathcal{L}\Delta t}{2(\Delta y)^2}; \mathcal{B}_4 = \frac{9\Delta t}{4}\, sin(x(i))cos(x(i));\\
&\mathcal{B}_5 = \frac{M\Delta t}{2}; \mathcal{B}_6 = \frac{3M\Delta t}{2}\, sin(x(i));\\
&\mathcal{B}_7 = \frac{\lambda\Delta t}{2}\, sin(x(i)); \mathcal{C}_3 = \frac{\mathcal{K}\Delta t}{2P_r(\Delta y)^2};
\end{aligned}$$

$$\mathcal{L} = \frac{1}{(1-\chi)^{2.5}\left((1-\chi) + \chi\left(\frac{\rho_s}{\rho_f}\right)\right)}$$

$$\mathcal{K} = \left(\frac{(k_s + 2k_f) - 2\chi(k_f - k_s)}{((k_s + 2k_f) + \chi(k_f - k_s))\left((1-\chi) + \left(\frac{\chi(\rho C_p)_s}{(\rho c_p)_f}\right)\right)}\right),$$

and the boundary and initial conditions are given below

$$\begin{aligned}
&\text{at } n = 0\\
&\quad u^0_{i,j} = 0, v^0_{i,j} = 0, T^0_{i,j} = 0,\\
&\text{at } n > 0\\
&\quad u^n_{i,0} = v^n_{i,0} = 0, T^n_{i,0} = 1 \text{ at } j = 0,\\
&\quad u^n_{i,N_y} = u_e(x), v^n_{i,N_y} = 0, T^n_{i,N_y} = 0 \text{ at } j = N_y.
\end{aligned}$$

We further rearrange the finite difference equations (27)-(29) into the following form

$$\begin{aligned}
&\mathcal{D}_1 u^{n+1}_{i,j-1} + \mathcal{E}_1 u^{n+1}_{i,j} + \mathcal{F}_1 u^{n+1}_{i,j+1} = \mathcal{G}_1,\\
&\mathcal{D}_2 T^{n+1}_{i,j-1} + \mathcal{E}_2 T^{n+1}_{i,j} + \mathcal{F}_2 T^{n+1}_{i,j+1} = \mathcal{G}_2,\\
&v^{n+1}_{i,j} = \mathcal{G}_3,
\end{aligned} \tag{30}$$

where

$$\begin{aligned}
&\mathcal{D}_1 = -\mathcal{B}_2 - \mathcal{B}_3; \mathcal{E}_1 = 1 + \mathcal{B}_1 + 2\mathcal{B}_3 - \mathcal{B}_5; \mathcal{F}_1 = \mathcal{B}_2 - \mathcal{B}_3;\\
&\mathcal{G}_1 = (1 + \mathcal{B}_5)u^n_{i,j} + \mathcal{B}_1(u^{n+1}_{i-1,j} + u^n_{i-1,j} - u^n_{i,j}) +\\
&\qquad \mathcal{B}_2(u^n_{i,j-1} - u^n_{i,j+1}) + \mathcal{B}_7(T^{n+1}_{i,j} + T^n_{i,j}) +\\
&\qquad \mathcal{B}_3(u^n_{i,j-1} - 2u^n_{i,j} + u^n_{i,j+1}) + \mathcal{B}_4 - \mathcal{B}_6;\\
&\mathcal{D}_2 = -\mathcal{C}_2 - \mathcal{C}_3; \mathcal{E}_2 = 1 + \mathcal{C}_1 + 2\mathcal{C}_3; \mathcal{F}_2 = \mathcal{C}_2 - \mathcal{C}_3;\\
&\mathcal{G}_2 = T^n_{i,j} + \mathcal{C}_1(T^{n+1}_{i-1,j} + T^n_{i-1,j} - T^n_{i,j}) +\\
&\qquad \mathcal{C}_2(T^n_{i,j-1} - T^n_{i,j+1}) +\\
&\qquad \mathcal{C}_3(T^n_{i,j-1} - 2T^n_{i,j} + T^n_{i,j+1});\\
&\mathcal{G}_3 = v^{n+1}_{i,j-1} - v^n_{i,j} + v^n_{i,j-1} -\\
&\qquad \mathcal{A}\begin{pmatrix} u^{n+1}_{i,j} - u^{n+1}_{i-1,j} + u^n_{i,j} - u^n_{i-1,j} +\\ u^{n+1}_{i,j-1} - u^{n+1}_{i-1,j-1} + u^n_{i,j-1} - u^n_{i-1,j-1}\end{pmatrix} -\\
&\qquad \Delta y\left(u^{n+1}_{i,j} + u^n_{i,j}\right) cot\,(x)\,.
\end{aligned}$$

which gives the following two tri-diagonal matrices for $i = 0, 1, 2, ..., N_x$ and $j = 0, 1, 2, ..., N_y$.

$$\begin{bmatrix}
\mathcal{E}_1 & \mathcal{F}_1 & 0 & 0 & \cdots & 0\\
\mathcal{D}_1 & \mathcal{E}_1 & \mathcal{F}_1 & 0 & \cdots & 0\\
0 & \mathcal{D}_1 & \mathcal{E}_1 & \ddots & \cdots & \vdots\\
0 & 0 & \ddots & \ddots & \mathcal{F}_1 & 0\\
\vdots & \vdots & \vdots & \mathcal{D}_1 & \mathcal{E}_1 & \mathcal{F}_1\\
0 & 0 & \cdots & 0 & \mathcal{D}_1 & \mathcal{E}_1
\end{bmatrix}
\begin{bmatrix}
u^{n+1}_{i,1}\\ u^{n+1}_{i,2}\\ u^{n+1}_{i,3}\\ \vdots\\ u^{n+1}_{i,N_y-2}\\ u^{n+1}_{i,N_y-1}
\end{bmatrix} \tag{31}$$

$$= \begin{bmatrix}
\mathcal{G}_1\\ \mathcal{G}_1\\ \mathcal{G}_1\\ \vdots\\ \mathcal{G}_1\\ \mathcal{G}_1
\end{bmatrix} + \begin{bmatrix}
u^{n+1}_{i,0}\\ 0\\ 0\\ \vdots\\ 0\\ u^{n+1}_{i,N_y}
\end{bmatrix}.$$

$$\begin{bmatrix}
\mathcal{E}_2 & \mathcal{F}_2 & 0 & 0 & \cdots & 0\\
\mathcal{D}_2 & \mathcal{E}_2 & \mathcal{F}_2 & 0 & \cdots & 0\\
0 & \mathcal{D}_2 & \mathcal{E}_2 & \ddots & \cdots & \vdots\\
0 & 0 & \ddots & \ddots & \mathcal{F}_2 & 0\\
\vdots & \vdots & \vdots & \mathcal{D}_2 & \mathcal{E}_2 & \mathcal{F}_2\\
0 & 0 & \cdots & 0 & \mathcal{D}_2 & \mathcal{E}_2
\end{bmatrix}
\begin{bmatrix}
T^{n+1}_{i,1}\\ T^{n+1}_{i,2}\\ T^{n+1}_{i,3}\\ \vdots\\ T^{n+1}_{i,N_y-2}\\ T^{n+1}_{i,N_y-1}
\end{bmatrix} \tag{32}$$

$$= \begin{bmatrix}
\mathcal{G}_2\\ \mathcal{G}_2\\ \mathcal{G}_2\\ \vdots\\ \mathcal{G}_2\\ \mathcal{G}_2
\end{bmatrix} + \begin{bmatrix}
T^{n+1}_{i,0}\\ 0\\ 0\\ \vdots\\ 0\\ T^{n+1}_{i,N_y}
\end{bmatrix}.$$

Then, the above tri-diagonal matrices (31) and (32) can be represented as the following tri-diagonal matrix.

$$\begin{bmatrix}
p_1 & s_1 & 0 & 0 & \cdots & 0\\
r_2 & p_2 & s_2 & 0 & \cdots & 0\\
0 & r_3 & p_3 & \ddots & \cdots & \vdots\\
0 & 0 & \ddots & \ddots & s_{N-2} & 0\\
\vdots & \vdots & \vdots & r_{N-1} & p_{N-1} & s_{N-1}\\
0 & 0 & \cdots & 0 & r_N & p_N
\end{bmatrix}
\begin{bmatrix}
v_1\\ v_2\\ v_3\\ \vdots\\ v_{N-1}\\ v_N
\end{bmatrix} = \begin{bmatrix}
w_1\\ w_2\\ w_3\\ \vdots\\ w_{N-1}\\ w_N
\end{bmatrix},$$

and by elementary row operations, one has

$$\begin{bmatrix}
p_1^{'} & s_1 & 0 & 0 & \cdots & 0\\
0 & p_2^{'} & s_2 & 0 & \cdots & 0\\
0 & 0 & p_3^{'} & \ddots & \cdots & \vdots\\
0 & 0 & \ddots & \ddots & s_{N-2} & 0\\
\vdots & \vdots & \vdots & 0 & p_{N-1}^{'} & s_{N-1}\\
0 & 0 & \cdots & 0 & 0 & p_N^{'}
\end{bmatrix}
\begin{bmatrix}
v_1\\ v_2\\ v_3\\ \vdots\\ v_{N-1}\\ v_N
\end{bmatrix} = \begin{bmatrix}
w_1^{'}\\ w_2^{'}\\ w_3^{'}\\ \vdots\\ w_{N-1}^{'}\\ w_N^{'}
\end{bmatrix}.$$

which can be solved iteratively by applying the following formula.

$$\begin{aligned}
&p_1^{'} = p_1,\ w_1^{'} = w_1,\ p_i^{'} = p_i - s_{i-1}\frac{r_i}{p_{i-1}^{'}},\\
&w_i^{'} = w_i - w_{i-1}^{'}\frac{r_i}{p_{i-1}^{'}},\ \text{for } i = 2, 3, ..., N,
\end{aligned}$$

and

$$\begin{aligned}
&v(N) = \frac{w^{'}(N)}{p^{'}(N)},\ v(i) = \frac{w^{'}(i) - s(i)v(i+1)}{p^{'}(i)},\\
&\text{for } i = N-1, N-2, ..., 2, 1.
\end{aligned}$$

Figure 2 shows that the velocity is increased in range of boundary layer thickness from $y = 0$ to $y = 1$ and is decreased in range of boundary layer thickness from $y = 1$ to $y = 5$. In the variation of the Prandtl number, the velocity profile becomes smaller when the Prandtl number is increased. This is due to the correlation among Prandtl number, kinematic viscosity, and thermal diffusivity. The Prandtl number is directly proportional to the kinematic viscosity and inversely proportional to the thermal diffusivity. The greater the Prandtl

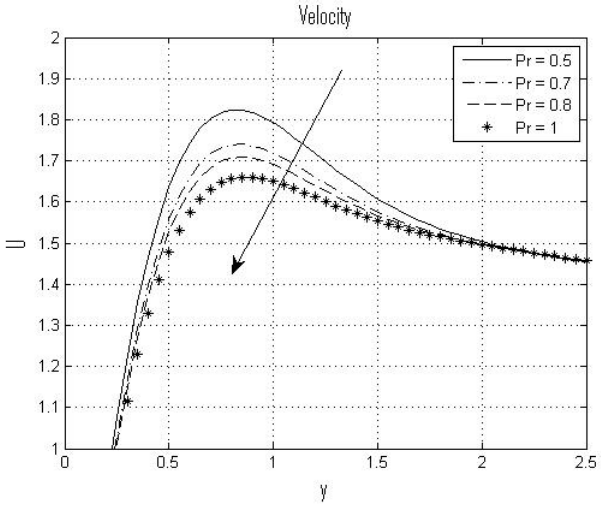

Fig. 2. Velocity profile with various Prandtl numbers

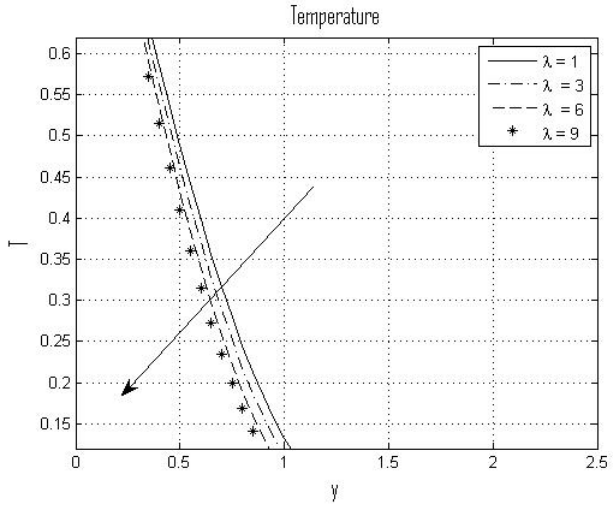

Fig. 5. Temperature profile with various mixed convection

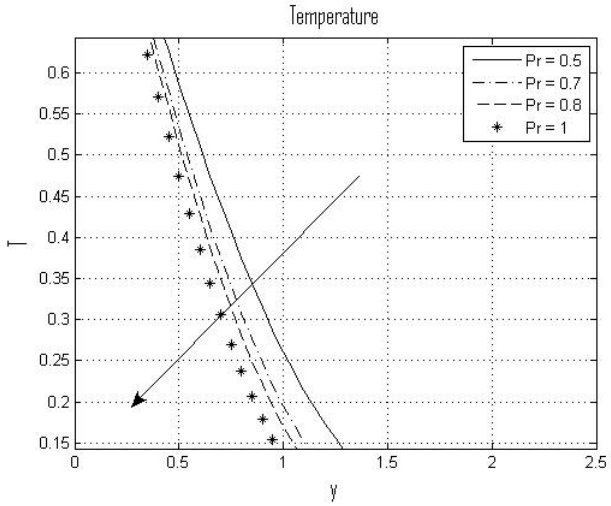

Fig. 3. Temperature profile with various Prandtl numbers

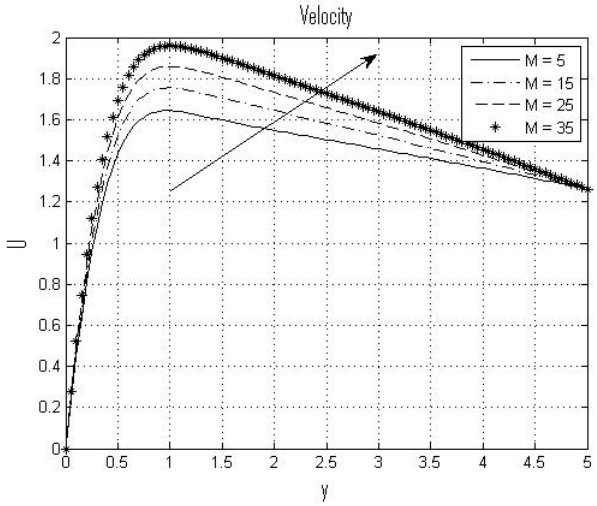

Fig. 6. Velocity profile with various magnetohydrodynamics

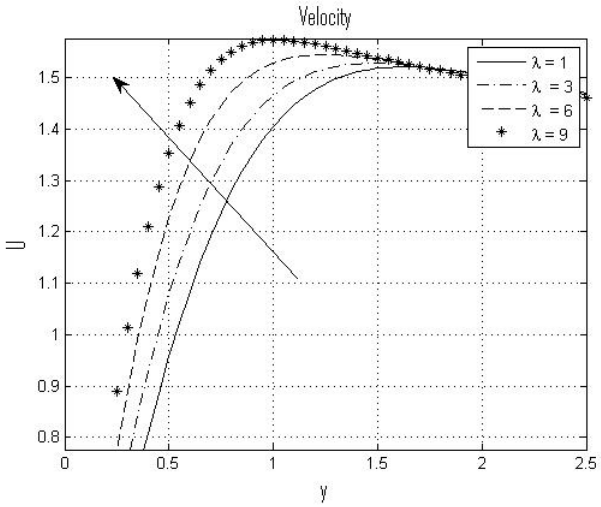

Fig. 4. Velocity profile with various mixed convection

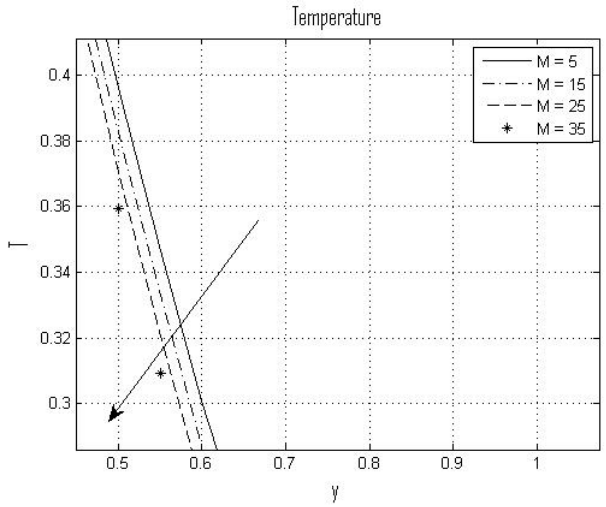

Fig. 7. Temperature profile with various magnetohydrodynamics

number, the greater the kinematic viscosity of the fluid so that the viscosity (*density*) of the fluid increases. As a result of increasing the viscosity (*density*) of the fluid, it causes the fluid flow velocity to decrease.

Figure 3 is decreased in the temperature profile of the nanofluid by the increases of boundary layer thickness from $y = 0$ to $y = 5$. In the variations of the Prandtl number, the temperature profile becomes smaller when the Prandtl number is increased. Mathematically, it can be written as follows

$$Pr = \frac{v\rho c_p}{k}$$

This means that the Prandtl number is the ratio between the kinematic viscosity and the thermal diffusivity. Thermal diffusivity is related to the ratio between the thermal conductivity of the fluid and the energy storage capacity so that the Prandtl number is inversely proportional to the thermal diffusivity. This results in a large increase in the Prandtl number, the lower the thermal diffusivity value of the fluid, resulting in a smaller profile temperature.

Figure 4 shows that the velocity is increased in range of boundary layer thickness from $y = 0$ to $y = 1$ and is decreased in range of boundary layer thickness from $y = 1$ to $y = 5$. In the variations of mixed convection parameters, the nanofluid velocity profile becomes larger when the convection parameters of the mixture are increased. This happens because the Reynolds number is proportional to the density of the fluid so that the convection parameter value of the mixture is inversely proportional to the density of the fluid. The greater the convection parameter of the mixture given, the lower the fluid density. The lower the density of the fluid, the greater the velocity of the fluid.

Meanwhile, Figure 5 is decreased in the temperature profile by the increases of boundary layer thickness from $y = 0$ to $y = 5$. In the variations of mixed convection parameters, the temperature profile of the nanofluid becomes smaller as the convection parameters of the mixture increase. This is because the convection parameters of the mixture are proportional to the temperature of the fluid so that the increasing of the convection parameters of the mixture causes the temperature of the fluid flow to be smaller.

Figure 6 shows that the velocity is increased in range of boundary layer thickness from $y = 0$ to $y = 1$ and is decreased in range of boundary layer thickness from $y = 1$ to $y = 5$. In the various parameters of magnetic, the fluid velocity profile becomes greater when the parameters of magnetic are increased. Because of the Lorentz force on the surface of sphere, then the fluid passing through the magnetic sphere receives the Lorentz force. Mathematically, Lorentz style is written as $\mathbf{F}$=$\mathbf{J} \times \mathbf{B}$ or $\mathbf{F}$=$\sigma(\mathbf{V} \times \mathrm{B} \times \mathrm{B})$, with $\mathbf{B}$=B_0 so that $\mathbf{F} \sim B_0$. The magnetic parameter is also proportional to B_0 or $M \sim B_0$ so that as the magnetic parameter increases, the value of B_0 increases. As the consequence, the Lorentz force on the surface of sphere also increases so that the effect on the fluid velocity becomes greater when the magnetic parameter is increased.

Figure 7 is decreased in the temperature profile of the nanofluid by the increases of boundary layer thickness from $y = 0$ to $y = 5$. In the variations of magnetic parameters, the fluid temperature becomes smaller as the magnetic parameters increase. The magnetic field generated by the magnetized sphere will cause the internal energy decreased so that it also causes the fluid temperature decreased.

III. Conclusions

Based on the results and discussions, the summaries of this paper are: The velocity profile is decreased when the variations of Prandtl numbers are increased. Meanwhile, the velocity profiles are increased when the variations of mixed convection and magnetohydrodynamics are increased. The temperature profiles are decreased for all variations of Prandtl numbers, mixed convection and magnetohydrodynamics. The Prandtl number is directly proportional to the kinematic viscosity and inversely proportional to the thermal diffusivity. The convection parameter value of the mixture is inversely proportional to the density of fluid. The magnetic parameter and Lorentz force are proportional to B_0 ($(\mathbf{F},\mathrm{M}) \sim B_0$).

References

[1] M. Tafrikan, B. Widodo, and C. Imron, "Pemodelan pengaruh panas terhadap aliran fluida konveksi bebas yang melalui bola berpori," 2015.

[2] I. Anggriani, B. Widodo, and C. Imron, "Magnetohydrodynamic in micropolar fluid through porous sphere," *Proceeding of The 6th Annual Basic Science*, 2016.

[3] A. Khan, M. Ashraf, A. M. Rashad, and H. A. Nabwey, "Impact of heat generation on magneto-nanofluid free convection flow about sphere in the plume region," *Mathematics*, vol. 8, no. 11, p. 2010, 2020.

[4] B. Widodo, D. K. Arif, D. Aryany, N. Asiyah, F. A. Widjajati, and Kamiran, "The effect of magnetohydrodynamic nano fluid flow through porous cylinder," in *AIP Conference Proceedings*, vol. 1867, no. 1. AIP Publishing LLC, 2017, p. 020069.

[5] Y. Norasia and Z. Zulaikha, "Pengaruh partikel nano zn dan zno terhadap aliran mhd fluida nano pada lapisan batas bola bermagnet," *Square: Journal of Mathematics and Mathematics Education*, vol. 1, no. 2, pp. 133–142, 2019.

[6] Y. Norasia, B. Widodo, and D. Adzkiya, "Pergerakan aliran mhd ag-air melewati bola pejal," *Limits: Journal of Mathematics and Its Applications*, vol. 18, no. 1, pp. 15–21, 2021.

[7] T. Morenike Agbaje and G. Makanda, "Numerical solutions for laminar boundary layer nanofluid flow along with a moving cylinder with heat generation, thermal radiation, and slip parameter," 2021.

[8] T. Agbaje and P. Leach, "Numerical investigation of natural convection viscoelastic jeffreys nanofluid flow from a vertical permeable flat plate with heat generation, thermal radiation, and chemical reaction," in *Abstract and Applied Analysis*, vol. 2020. Hindawi, 2020.

[9] W. Jamshed, "Numerical investigation of mhd impact on maxwell nanofluid," *International Communications in Heat and Mass Transfer*, vol. 120, p. 104973, 2021.

[10] M. Prameela, D. V. Lakshmi, and J. R. Gurejala, "Influence of thermal radiation on mhd fluid flow over a sphere," 2021.

[11] W. Khan, Z. Khan, and R. U. Haq, "Flow and heat transfer of ferrofluids over a flat plate with uniform heat flux," *The European Physical Journal Plus*, vol. 130, no. 4, pp. 1–10, 2015.

[12] A. Zeeshan, A. Majeed, and R. Ellahi, "Effect of magnetic dipole on viscous ferro-fluid past a stretching surface with thermal radiation," *Journal of Molecular liquids*, vol. 215, pp. 549–554, 2016.

[13] A. Sahaya Jenifer, P. Saikrishnan, and R. W. Lewis, "Unsteady mhd mixed convection flow of water over a sphere with mass transfer," *Journal of applied and computational mechanics*, vol. 7, no. 2, pp. 935–943, 2021.

[14] B. Widodo, Y. Norasia, and D. Adzkiya, "Mhd fluid flow with the effect of mixed convection passing on a magnetic sphere in newtonian nano fluid," in *Journal of Physics: Conference Series*, vol. 1218, no. 1. IOP Publishing, 2019, p. 012057.

[15] M. Ghani, "Numerical results of mixed convection flow over a flat plate with the imposed heat and angle of inclination," *Euler: Jurnal Ilmiah Matematika, Sains dan Teknologi*, vol. 9, no. 2, pp. 85–93, 2021.

[16] M. Ghani and W. Rumite, "Keller-box scheme to mixed convection flow over a solid sphere with the effect of mhd," *MUST: Journal of Mathematics Education, Science and Technology*, vol. 6, no. 1, pp. 97–120, 2021.